Tellus (1996), 48B, 329–346
Printed in UK – all rights reserved

TELLUS
ISSN 0280–6509

On a two-dimensional energy balance climate model coupled interactively to a land carbon cycle model

By Y.-H. CHAN[1], D. CHAN[2], and K. HIGUCHI[2]*, [1]*Western Ecological Services Ltd., 2–2563 Penrhyn Street, Victoria, B.C., Canada V8N 1G2;* [2]*Atmospheric Environment Service, 4905 Dufferin Street, Downsview, Ontario, Canada M3H 5T4.*

(Manuscript received 8 february 1994; in final form 27 November 1995)

ABSTRACT

A two-dimensional (latitude-height) climate/global carbon cycle model has been developed to investigate the interactive climate/biogeochemical response of a land biosphere to a linearly increasing input of carbon totalling 1000 Gtons C into the atmosphere over a 150-year period. With no fertilization response to the increasing CO_2 content in the atmosphere (fertilization factor = 0.0), the land biosphere acts as a net source of CO_2 for the atmosphere. This is mainly due to the soil carbon response to increasing surface temperatures, resulting in a greater soil release than the uptake of carbon by NPP. At the end of 150 years, globally averaged NPP has increased by about 2.3 Gtons C yr^{-1}, while the soil respiration has increased by 3.9 Gtons C yr^{-1}. When the land biosphere is allowed to respond to the increasing atmospheric CO_2 (fertilization factor = 0.3), NPP increases at a much faster rate than the soil release, causing the land biosphere to become a net sink for the excess CO_2 in the atmosphere. In this case, NPP has increased by about 15.4 Gtons C yr^{-1}, while the soil release has increased by around 12.9 Gtons C yr^{-1}.

1. Introduction

The concentration of atmospheric CO_2 has been increasing steadily since the beginning of the industrial era. Records of atmospheric CO_2 from several background monitoring stations around the world reveal that the increasing trend will likely continue into the near future, and the concentration will double to about 600 ppmv (parts per million by volume) by the middle of the next century (IPCC, 1990), causing some major climatic changes to occur. To increase our understanding of the climatic change, we first need to obtain an adequate understanding of the complex interaction between the physical climate and the global carbon cycle, because some of the biogeochemical processes within the carbon cycle are climate dependent. For example, changes in the earth's climate parameters such as temperature and precipitation are expected to affect the physiological responses of land plants, leading to changes in the carbon budgets of the terrestrial biosphere (Olson et al., 1978). It is therefore of great interest to obtain an estimate of the significance of the impact of changes in the terrestrial carbon cycling brought about by changing climate, on the future evolution of the atmospheric CO_2 concentration levels.

Various models of different simplification of the global carbon cycle have been used to simulate the increase of atmospheric CO_2, and to project future concentrations resulting from fossil fuel emissions (SCOPE 16, 1981). In many of these models, the terrestrial biosphere is either ignored or divided into several carbon pools. Emanuel et al. (1985), for example, have produced, using

* Corresponding author.

the Holdridge life-zone classification system, different maps of plant community distribution of the world under $1 \times CO_2$ and $2 \times CO_2$ temperature and moisture regimes. Uchijima and Seino (1988a,b) have employed the Chikugo model (Uchijima and Seino, 1985) and the climatic scenario produced by the Goddard Institute of Space Science (GISS) to study probable changes in the agroclimatic resources and net primary productivity (NPP) of the natural vegetation in Japan. Seino and Uchijima (1992) then used the model to estimate NPP of terrestrial vegetation on a global scale. These and many of the other terrestrial carbon cycle models used in models of the global carbon cycle represent a one-way response to a climatic change, with no feedback to the climate system (see, for example, Harvey (1989)).

In a recent study to understand the two-way interaction between the changes in the physical aspects of the climate system and the biogeochemical processes of the global carbon cycle, Rotmans and Den Elzen (1993) have developed a globally averaged multi-box coupled climate/carbon cycle model. Their study points to the importance of the fertilization factor in NPP in determining the future levels of the atmospheric CO_2. Its implication is important because of the potential role of the land biosphere in the "missing carbon" issue (Tans et al., 1991).

In this study, we extend the modelling effort of Rotmans and Den Elzen (1993) and test the robustness of some of their sensitivity results. To investigate the transient response of the land carbon content to changes in the climate parameters and atmospheric CO_2 content, we have used an empirical global land biosphere model coupled to a two-dimensional zonally-averaged multilayer energy balance climate model (Chan et al., 1995) with an incorporated carbon transport equation. Marine carbon cycle is not considered here, but will be addressed in a later study. We present preliminary results of incorporating the Chikugo NPP formulation into the terrestrial carbon cycle model that also considers plant litterfalls and probable shifts in soil carbon.

We briefly describe the coupled climate/land carbon cycle model in Section 2, followed in Section 3 by a discussion of the results of the land biosphere model response to an increasing atmospheric CO_2 concentration for fertilization factors of 0.0 and 0.3. We conclude with a brief summary in Section 4.

2. Model description

In this section we briefly describe the features of the individual components which constitute the coupled model.

2.1. *Atmosphere and ocean*

The physical climate model used in this study is based on the model developed by Peng et al. (1987), and is composed of a 2-dimensional (latitude-height) zonally averaged multilayer energy balance atmospheric component coupled interactively to a 1-dimensional (north-south) mixed layer ocean of 95-m thickness. Only a cursory description of the model will be given here, and the reader is referred to Peng et al. (1987) and Chan et al. (1995) for a more detailed description.

The atmospheric component is divided into eighteen 10-degree latitude zones in the meridional direction from 90°S to 90°N, and 5 dynamical layers in the vertical direction from pressure $p =$ 1000 mb to 0 mb with equal pressure spacing of 200 mb. There are 6 radiative layers in each of the lower 4 dynamical layers (troposphere) and 4 radiative layers in the upper most dynamical layer (stratosphere). The radiation code is adapted from Blanchet and Morcrette (1985). The model is integrated using a finite differencing scheme, with a time step of 6 hours. The relative humidity field is prescribed with the observed seasonal distribution. The only prognostic variable is temperature. The atmospheric temperature (T_{air}) is governed by

$$C_p \frac{\partial T_{air}}{\partial t} = H_{SR} + H_{IR} + H_{LH} + H_{LSE} + H_{SSE} + H_{MMC} \quad (1)$$

where C_p is the heat capacity of the atmosphere and H is the heat convergence; the subscripts SR, IR, LH, LSE, SSE and MMC denote solar radiation, infrared radiation, latent heat, large scale eddies, small scale eddies, and mean meridional circulation, respectively.

The earth's surface in each latitude zone is divided into 3 types: land, ocean, and sea ice. The energy balance for these 3 surface types are given

by:

$$\rho_L C_L D_L \frac{\partial T_L}{\partial t} = S_L + I_L + SH_L + LE_L, \quad (2)$$

$$\rho_W C_W D_W \frac{\partial T_W}{\partial t} = S_W + I_W + SH_W + LE_W + COF - FWI, \quad (3)$$

$$\rho_I C_I D_I \frac{\partial T_I}{\partial t} = S_I + I_I + SH_I + LE_I + FI + \frac{FWI(1-AI)}{AI}. \quad (4)$$

Here, ρ, C, and D are the density, heat capacity and depth of heat capacity layer, respectively. The subscripts L, W, and I refers to land, open water, and sea ice, respectively. The forcing functions S, I, SH, and LE are the downward surface fluxes of solar radiation, infrared radiation, sensible heat, and latent heat, respectively, at the surface. COF is the horizontal heat convergence in the ocean mixed layer, FWI is the lateral heat transfer from the open ocean area to the sea ice, FI is the upward conduction in sea ice, and AI is the fraction of ocean covered by ice. The zonal surface temperature is computed from the fractional area of these 3 surface types. However, the only temperature the land biosphere responds to is the surface land temperature, T_L.

Carbon in the atmosphere is transported with the same diffusive coefficients used to transport energy in the atmosphere. These coefficients represent large and small scale eddy transports, and are a function of spatial potential temperature gradients (Peng et al., 1987).

The oceanic component, to which the atmospheric component is connected interactively, is represented by a mixed layer of 95-metre thickness, in which an annual climatological poleward heat transport is specified. The data are obtained from Newton (1972). There is no physical poleward water movement in the layer. Marine carbon cycle is not included in the oceanic component, as our focus in this study is the interactive effect of climatic change on the terrestrial carbon cycle.

For an average CO_2 concentration of 334 ppm in the atmosphere, the difference between the simulated and observed annual temperature field is shown in Fig. 1. Because of the more zonal nature of the climate processes in the southern hemisphere, the model results are much closer to the observation there than in the northern hemisphere. Overall there is a very good qualitative agreement between the model results and the observation. Latitudinally averaged annual mean net radiation balance calculated by the model for the surface is compared to an observation in Fig. 2. Here too, the overall agreement between the model calculation and the observation is good, although the model does slightly overestimate the net radiation in the tropical region. As will be described in subsection 2.2, these two climate parameters, the surface temperature and the net radiation, are the terms in the equation to calculate the net primary productivity in the land carbon cycle model.

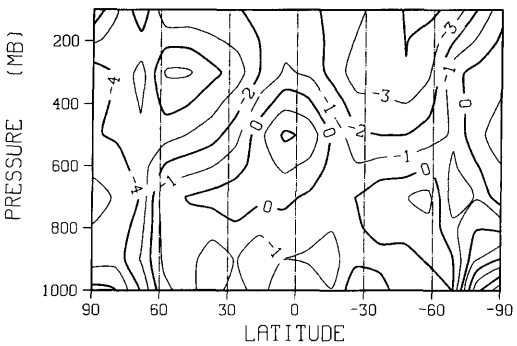

Fig. 1. Difference between the simulated and observed zonally averaged annual temperature field (°C).

The climate parameters used as inputs to the land biosphere model are the 10° zonal averages of daily net radiation and ground-level temperature. A time step of 0.25 day is used for the climate model, while a time step of 1 day is used

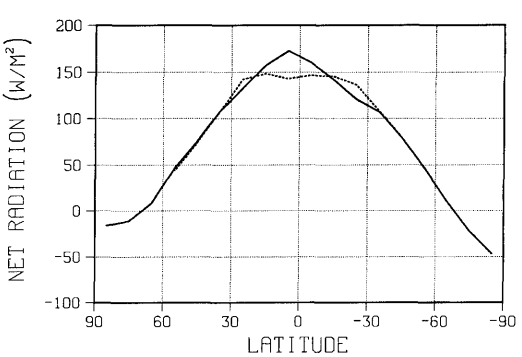

Fig. 2. Calculated (solid) values of latitudinally averaged surface net radiation, compared to the observed (dash) values (Schutz and Gates, 1974).

for the land biosphere carbon cycle model. In this study we focus on the change in the carbon content of the model land biota in its interactive responses to changing physical climate and atmospheric carbon reservoir size.

2.2. *Land biosphere*

The carbon budget of the biospheric component is calculated with a simple two-reservoir model. One reservoir represents the phytomass carbon (Cb) and the other, the soil carbon (Cs). Uptakes of CO_2 by land vegetation are estimated from the net primary production (NPP) of different plant ecosystems. Carbon is transferred from the phytomass reservoir to the soil reservoir by root turnover and litterfall (LF). The return fluxes of CO_2 to the atmosphere from the soil reservoir are estimated from various empirical relationships between ground level temperature and emissions of soil CO_2 (F_{sr}). The equations are as follows:

$$\mathrm{Cb}(t)=\mathrm{Cb}(t-1)+[\mathrm{NPP}(t)-\mathrm{LF}(t)]\Delta t \tag{5}$$

$$\mathrm{Cs}(t)=\mathrm{Cs}(t-1)+[\mathrm{LF}(t)-F_{\mathrm{sr}}(t) \times(1-\text{root respiration})]\Delta t. \tag{6}$$

We make an assumption that there would be no significant movement of ecosystem boundaries resulting from the levels of climatic changes simulated by the model on a 100-year time scale. A dominant response of each ecosystem to climate warming, instead, would be changes in its carbon content. Major aspects of the land biosphere model are now described below.

2.2.1. Vegetation carbon. The land vegetation is divided into 33 ecosystem complexes as given by Olson et al. (1983). The total area of vegetated land occupies about 132×10^6 km^2, which is about 26% of the total area of the earth. The remaining 379×10^6 km^2 of the earth's surface is assigned to the Antarctica, ice cover and water. Within each 10° latitude zone, the number of 0.5 by 0.5 degree cell is enumerated from the database compiled by Olson et al. (1985). The number of cells is then converted to surface area. Although we have resolved the land biosphere into 33 individual ecosystem complexes, the two dimensional structure of the climate model allows discussion of carbon content changes in the land biosphere only on the zonal basis.

2.2.2. Net primary production. Uptake of CO_2 within each 10° latitude zone is defined as the sum of the NPPs of all the ecosystems found within the zone. In our study, the NPP of different ecosystem complexes are estimated with the semi-empirical Chikugo model (Uchijima and Seino, 1985; 1988). Uchijima and Seino (1985) have derived a functional relationship of dry-matter production from consideration of turbulent diffusion of water vapour and CO_2 due to transpiration as well as photosynthesis of plant community. The relationhip suggests that NPP can be approximated as a multiplicative product of the net radiation (Rn) and an energy conversion coefficient (α). The latter term itself is a function of the water deficit of air, the Bowen ratio, and a constant relating to diffusion conditions and CO_2 concentrations between the plant community and the surface air layer (Seino and Uchijima, 1992).

There is not enough information to estimate the coefficient α, but its value may be estimated from other climatic variables, especially the radiative dryness index (RDI), which is defined as the ratio of annual net radiation to the product of annual precipitation and latent heat of evaporation. Using about 700 sets of NPP and climatic data grouped in each RDI-band of a width of 0.2 from various parts of the world, Uchijima and Seino (1985) were able to verify the linear relationship between NPP and Rn, and thus obtain estimates of the coefficient α. Furthermore, they were also able to obtain an estimating equation for the coefficient from the corresponding RDI and showed that the coefficient decreases exponentially with increasing RDI. Thus, the original Chikugo model for estimating NPP from climatic data is given by:

$$\mathrm{NPP}=0.29[\exp\{-0.216(\mathrm{RDI})^2\}]\,\mathrm{Rn}. \tag{7}$$

To verify the Chikugo model, Seino and Uchijima (1985, 1988) used the model to assess intensively the NPP in Japan. Their assessments of the total NPP in Japan annually and for the growing seasons agree well with the results obtained from plant ecological methods. Furthermore, using published records from more than 1100 weather stations around the world, Uchijima and Seino (1992) have also produced global distribution maps of terrestrial NPP from the Chikugo model. According to Seino and Uchijima (1992), their maps of global NPP agree in general with Lieth's Miami Model map (Lieth, 1975) and the global

NPP map produced by Efimova (1976). However, there are also some differences; for example, the extremely high NPP of 25–30 t DM ha^{-1} yr^{-1} estimated by the Chikugo model covers a considerably smaller area than the other NPP distribution maps (Seino and Uchijima, 1992).

A slight modification of the Chikugo model is used in our study to take into account the possible fertilization effect of ambient CO_2. The modified equation is thus given as:

$$\mathrm{NPP}=0.29[\exp\{-0.216(\mathrm{RDI})^2\}] \times \mathrm{Rn}\,[1+\beta \ln(C(t)/C(0))], \quad (8)$$

where β is the fertilization factor or "biotic growth factor" (Kohlmaier et al., 1987; Keeling, 1973), and is assigned a value of either 0 or 0.3 in our experiments to be described in the next section. The variable $C(t)$ is the atmospheric CO_2 concentration at time t, and C(0) is the atmospheric CO_2 concentration at the beginning of a model simulation.

In our study, the average Rn of land surface from each 10° latitudinal zone is obtained from the 2-dimensional multilayer energy balance climate model already described above, and the RDI of each ecosystem complex is assigned according to the results of Budyko (1974) and Uchijima and Seino (1988). Since the Chikugo model has been developed to estimate the maximum potential of NPP, several adjustments are required to obtain the appropriate NPP of existing vegetation. Although the classification of Olson et al. (1983) allows for several types of cultivated lands, partial reduction in cultivated land has also occurred in areas classified as natural ecosystem complexes. The fraction of natural vegetation on each $1° \times 1°$ cell compiled by Matthews (1983) is used to adjust the deterioration of the natural vegetation cover. Adjustments for NPP of cultivated lands follow the values suggested by Uchijima and Seino (1988a). Several of the ecosystem complexes also require further adjustment for altitudinal effect, since NPP is reduced by decreasing temperature at high altitude (Leith, 1975; Uchijima and Seino, 1985). These ecosystems include alpine components of tundra, wooded tundra, taiga, and southern taiga at low latitudes, the highland shrubs and the tropical mountain forests. Thus, the total NPP (TNP) in the jth-latitude zone is estimated by

$$\mathrm{TNP}_j=\sum_k \mathrm{NPP}_{jk}A_{jk}V_{jk}E_{jk}, \quad (9)$$

where NPP_{jk} is the NPP of the kth ecosystem complex estimated from the Chikugo model, A_{jk} is the area of the kth ecosystem complex in the latitude zone, V_{jk} is the fraction of natural vegetation in the kth ecosystem complex, and E_{jk} is the efficiency of NPP of the kth ecosystem complex to adjust for altitude and other factors.

Even though RDI is a function of Rn and precipitation (both of which are calculated by the climate model), we have kept the RDI value of each ecosystem complex constant in this study. This constraint will be removed in our future studies with the 2-d climate/land carbon cycle model.

2.2.3. Root turnover and litterfall. The amount of annual litterfall and root turnover for all vegetation types are compiled from various reviews (Ajtay et al., 1979; Bray and Gorham, 1964; Vogt et al., 1986). To allow for a simulation time step of 1 day, these annual values are multiplied by an appropriate seasonality function to give the values on a daily basis. The litterfall values of various forests from Bray and Gorham (1964) are fitted to seasonal function of the form:

$$\begin{aligned} L&=a_1+(a_2t), && 0<t<\mathrm{t}_1,\\ L&=L_\mathrm{m}/\{[(t-t_\mathrm{m})/t_\mathrm{s}]^2+1\}, && t_1<t<\mathrm{t}_2,\\ L&=a_3+(a_4t), && t_2<t<365, \end{aligned} \quad (10)$$

where L is the fraction of the total annual litterfall on day t, L_m is the maximum fraction of the annual litterfall on day t_m, t_s is a constant to specify the extent of the litterfall period, and a_1 to a_4 are constants. The time parameters t_1 and t_2 denote the start of the autumn or dry-season litterfall and the end of the seasonal litterfall, respectively. These regression functions express seasonal litterfall variation for each of the ecosystems as a percentage or fractional function of the total annual litterfall.

A simple non-linear regression method was used to obtain estimates of the constants a_1 to a_4. The time variables, t_1 and t_2, and their corresponding fraction of annual litterfall are estimated directly from the figures of Bray and Gorham (1964). After the initial regression fitting, the values are adjusted iteratively to ensure that the total fraction for the 365 days add up to 1.0.

A total of 11 different seasonality functions have been used in the model. Five of these are restricted

to the northern hemisphere latitudes, another five to the southern hemisphere latitudes, and the remaining one function could be used for both northern and southern hemisphere latitudes (Appendix A). The seasonal variation in litterfall and root turnover of each ecosystem complex has been assigned to one of these functions. The annual litterfall of the individual ecosystem is made equal to its annual NPP of the previous year, thus guaranteeing no net change in the carbon content of the phytomass under steady state condition.

2.2.4. Soil carbon. The amount of soil carbon consists mainly of organic carbon in mineral soil and in the soil-surface detritus. A data set of worldwide organic soil carbon has been compiled by Zinke et al. (1984). Their summaries give the averages of soil carbon on most Holdridge life zones, as well as on Olson's ecosystem complexes. These averages are used in our model. The amount of detritus carbon for several vegetation types have been taken from various sources (Ajtay et al., 1979; Bray and Gorham, 1964; Schlesinger, 1977; Vogt et al., 1986).

2.2.5. CO_2 emission from soil. The CO_2 produced from root respiration and the microbial decomposition of soil carbon are assumed to be released to the atmosphere. Kempe (1979) has suggested that greater than 99% of the total CO_2 produced is released into the atmosphere. (The remaining portion becomes dissolved in ground water.) Since the release of CO_2 from root respiration has already been taken into account in the estimation of NPP, this fraction is subtracted from the total soil respiration to arrive at the amount of CO_2 released from the soil due to the microbial decomposition alone.

In many studies, soil respiration had been shown to vary with soil temperature, precipitation, evapotranspiration, soil moisture, or substrate quality (Singh and Gupta, 1973; Raich and Schlesinger, 1992). For our study, we have assumed that soil respiration (F_{sr}) can be adequately estimated as a first-order function of total soil carbon (C_{soil}). In addition, the proportionality "constant" relating the soil carbon to the soil respiration has been assumed to vary as an Arrhenius function of ground-surface temperature. That is:

$$F_{sr} = a \exp(b/T)\, C_{soil}, \qquad (11)$$

where a and b are constants, and T is the land-surface temperature in Kelvin. The constants a and b are obtained by regression method from data of soil respiration and ground temperature compiled from various published reports (Appendix B). Since the results in most of these reports are presented in a graphical form, these graphs have been digitized first to obtain numerical values of soil respiration and the corresponding ground temperature. If the amount of soil carbon is not reported for a particular vegetation type, then the average value for that vegetation type are obtained from Zinke et al. (1984). Finally, the calculated rate constant (F_{sr}/C_{soil}) is fitted to an Arrhenius-type equation to obtain the regression constants a and b for each of the soil types. In our study, 17 equations representing 16 different vegetation types are derived. Separate equations for the dry and wet seasons are used to estimate the rate of soil respiration of tropical seasonal forests and tropical savanna and woodlands (Appendix B). Under steady state condition, the annual carbon transferred from the soil to the atmosphere, i.e. the soil respiration, is made equal to the annual TNP of the individual ecosystem, by adjusting the soil carbon content slightly from the values obtained from the literature.

2.2.6. Steady state TNP and NEP. The equilibrium model simulations of the present-day latitudinally averaged seasonal TNP (as given by equation (9)) and net ecosystem productivity ($NEP = TNP - F_{sr}$), as driven by the climate model (Figs. 1, 2) with the globally averaged atmospheric CO_2 concentration of 334 ppm, are shown in Fig. 3 for $\beta = 0$.

The seasonal cycle of TNP simulated by the model in steady state is shown in Fig. 3a as a function of latitude. The overall result is in good agreement with the generalized monthly NPP produced by the model biosphere of Gillette and Box (1986), even though their model formulation is quite different from the one used in this study. Both models show a distinct maximum in NPP of about 1 Gtons C month^{-1} per 10° latitude zone in the high midlatitude region during the May/June period.

The seasonal evolution of the latitudinally averaged net ecosystem productivity (NEP) is shown in Fig. 3b. Net ecosystem productivity is the difference between TNP and F_{sr}, with positive

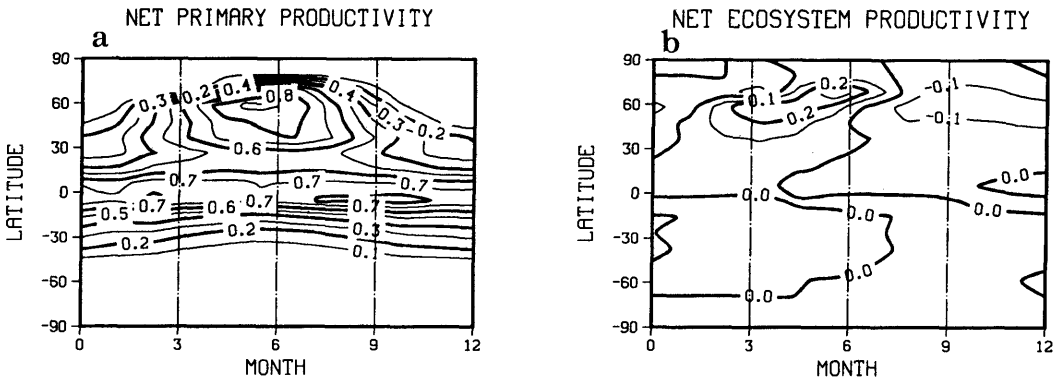

Fig. 3. Latitudinally averaged seasonal (a) total NPP (TNP) and (b) net ecosystem productivity (NEP) under steady state condition with $\beta=0$. Units are in Gtons C month^{-1} per 10° latitude zone.

values indicating net transfer of carbon from the atmosphere to the land biosphere. In comparing Fig. 3b with the global NEP values simulated by Gillette and Box (1986) and by Potter et al. (1993), there are very distinctive differences among these model results. First of all, the seasonal cycle of the latitudinally averaged global net carbon flux from the model biosphere used by Gillette and Box (1986) shows a maximum transfer of carbon from the atmosphere to the land biosphere at around 30°N during July and August, while the CASA-Biosphere model (Potter et al., 1993) shows a global NEP maximum around 60°N centred in July. The model used in this study, although less sophisticated than the one developed by Potter et al. (1993), shows a similar pattern in the NEP seasonal cycle as that of the CASA-Biosphere model in the high latitudes; one notable difference between the two models appears to be that the net primary productivity in the model used in this study starts quickly in April, before any significant seasonal release of CO_2 takes place, resulting in a first NEP maximum in April followed by the more pronounced second maximum at a slightly higher latitude in June (Fig. 3b). Also, the seasonality in NEP in the CASA-Biosphere model is quite pronounced in the tropical zones north and south of the equator. This noticeable seasonality is not evident in the model used in this study.

The lack of seasonality in NEP in the tropical region results from several factors. One of these is that NPP in the present model configuration is primarily driven by the net surface radiation (Rn), and does not respond to any seasonal changes in temperature and precipitation. However, wet and dry cycle is incorporated into the model as a function of seasonal temperature cycle (NPP=0 during the dry period). Another major factor is that the regression coefficients of the soil release equation (11) for each soil type are determined from the in-situ observed values of temperature and soil carbon content. The equation is then driven by the zonally averaged temperature of the 2-dimensional climate model. This loss of resolution mutes the seasonal variation of soil release in the tropical region. It has been shown that NEP is very sensitive to the assumed relationship between F_{sr} and temperature (Lloyd and Taylor, 1994).

Sensitivity of our results described in the section below to the seasonality of NEP in the tropical ecosystem complexes is tested by increasing the degree of responsiveness of NPP to the seasonal changes in the climate model's tropical temperature. This is achieved by increasing the amplitude response of NPP to the wet and dry cycle (parameterized as a function of seasonal temperature cycle) for such ecosystem as the seasonal tropical forest, and running the coupled climate/land carbon cycle model to an equilibrium. Preliminary analyses indicate that the results obtained from the numerical experiments discussed below in Section 3 are relatively invariant to the seasonality of NEP in the tropics. This is because, as will be shown, the carbon cycling on land is more responsive to perturbation in the atmospheric CO_2 concentration (through β effect) than to changes in the climate parameters.

3. Land biota response to increasing atmospheric CO_2

In this section, we discuss the results of two experiments to determine the sensitivity of the response of the land biosphere model (with different values of the CO_2 fertilization factor) to increasing atmospheric CO_2 concentration. This increase in the atmospheric CO_2 content is effected over a period of 150 model years from a steady state by a specified linearly increasing carbon input function (hereafter referred to as the "anthropogenic source") such that a total amount of 1000 Gtons C is released into the atmospheric

Table 1. *Carbon contents and fluxes in land biosphere*

Ecosystem complex	Area (10^6 km^2)	Biomass carbon (kg m^{-2})	RDI	Litterfall (kg m^{-2} yr^{-1})	Soil carbon (kg m^{-2})
1. main taiga	5.53	6	0.5	0.27	23.7
2. southern taiga	1.59	8	0.7	0.30	14.0
3. conifer forest	3.50	13	0.8	0.55	16.1
4. mixed forest	3.53	7	0.8	0.48	12.9
5. temp. broad-leaved	1.50	9	0.8	0.41	17.1
6. eq. evergreen	10.43	12	0.9	0.91	11.0
7. tropical seasonal	4.72	6	1.5	0.63	11.6
8. tropical savanna	6.72	3	2.2	0.41	6.2
9. tropical montane	1.18	6	1.3	0.61	19.2
10. succulent thorns	3.97	3	2.2	0.39	2.4
11. Mediterranean	1.01	3	1.3	0.48	7.8
12. highland shrub	2.61	3	1.7	0.29	8.0
13. semiarid woods	0.91	4	1.7	0.39	10.4
14. northern taiga	4.35	5	0.6	0.25	14.7
15. forest/field	5.17	4	1.3	0.58	7.7
16. field/woods	4.07	3	1.7	0.48	12.3
17. paddy land	1.98	3	1.0	0.25	14.7
18. irrigated cropland	1.58	2	1.3	0.45	7.3
19. cool cropland	2.97	0.7	1.3	0.30	10.4
20. warm cropland	9.29	0.8	1.7	0.25	9.6
21. cool grassland	3.94	0.8	2.0	0.28	12.6
22. warm grassland	17.30	0.9	2.2	0.30	8.9
23. heath, moors	0.15	1	1.7	0.27	16.1
24. cold rangeland	0.84	1	2.0	0.10	27.2
25. wooded tundra	1.74	2	0.4	0.15	19.1
26. tundra	9.47	0.5	0.3	0.12	18.4
27. cold desert	2.01	0.6	2.7	0.10	6.2
28. sand desert	5.21	0.1	3.5	0.10	3.4
29. hot desert	10.99	0.3	4.0	0.056	2.5
30. bogs, bog woods	0.97	2	0.6	0.41	178.4
31. warm wetlands	1.57	2	0.2	0.91	28.4
32. coastal edges	1.00	3	1.5	0.55	5.3
33. polar desert	0.54	0.07	3.5	0.013	4.8
Antarctic, ice	15.81	0	0	0	0
water	363.15	0	0	0	0

component at latitude zones 30–60°N. This gives an annual input of 0 Gtons C at $t=0$ to 13.34 Gtons C at $t=150$ years. If all the carbon stayed in the atmosphere, then the atmospheric CO_2 concentration would increase by about 470 ppm after 150 years.

Table 1 lists carbon contents and annual fluxes associated with the 33 ecosystems of the land biosphere model in steady state with the atmospheric CO_2 concentration of 334 ppm, with fertilization factor $\beta=0$ (Experiment I). Corresponding values for the case of fertilization factor $\beta=0.3$ (Experiment II) are very similar in magnitude. For both experiments, the model is initially integrated for 200 years until a satisfactory degree of steady state is obtained. Indeed, after 200 years of integration, the coupled model shows only a very small drift of 0.006 ppm yr^{-1} increase in the atmosphere, while the land biosphere shows an equivalent rate of decrease in carbon content. Within the context of the experiments described in this section, the model drift will have a negligible impact on the conclusions drawn from the results of the experiments.

A CO_2 fertilization factor of 0.0 is used in Experiment I, while 0.3 is used in Experiment II. Although the exact value of the fertilization factor is not know and remains quite controversial, we have decided to employ $\beta=0.3$, based on the studies by Harrison et al. (1993) and Kohlmaier et al. (1987). Global values of the coupled model parameters at $t=0$ and at $t=150$ years are summarized in Table 2 for the two experiments.

3.1. *Experiment I: fertilization factor* $\beta=0.0$

Latitudinal distribution of the annually averaged living phytomass carbon content, soil carbon content, and TNP are shown in Fig. 4a,b,c, respectively, for the steady state with zero fertilization factor. As noted in Ajtay et al. (1979), over 80% of the carbon content in the above ground land biota (living phytomass) resides in forests of different kind. This is reflected in Fig. 4a. Total carbon content in living phytomass is about 450 Gtons C, while that of the soil carbon content is around 1935 Gtons C. Much of this soil carbon resides in the extratropical northern hemisphere, with a large fraction north of 40°N. Considerable amount of carbon content of the tropical ecosystems lies above ground, which makes tropical deforestation a very important issue. The globally averaged value of TNP in the model is approximately 58 Gtons C yr^{-1}. On an annual basis, TNP is balanced by the soil respiration. Maximum TNP is observed in the equatorial region.

Fig. 5 shows the annually averaged temperature increase, relative to its initial steady state distribution (Fig. 1), after 150 years of the perturbed run. Warming near the surface in the polar latitudes is due to the ice albedo feedback, while the cooling in the stratosphere is caused by the enhanced

Table 2. *Global values at $t=0$ and $t=150$ years of model integration for Experiment I ($\beta=0$) and Experiment II ($\beta=0.3$)*

	Initial steady state						After 150 years of integration					
	TNP (Pg C per year)	F_{sr} (Pg C per year)	C_{ph} (Pg C)	C_s (Pg C)	τ_s (years)	T_s (°C)	ΔTNP (Pg C per year)	ΔF_{sr} (Pg C per year)	ΔC_{ph} (Pg C)	ΔC_s (Pg C)	τ_s (years)	ΔT_s (°C)
$\beta=0$	58.2	58.2	448.4	1934.5	33.2	13.7	2.3	3.9	17.3	−144.2	28.8	2.5
$\beta=0.3$	58.3	58.3	449.7	1935.7	33.2	13.7	15.4	12.9	108.8	103.4	28.6	1.9

TNP: total net primary productivity
F_{sr}: soil respiration
C_{ph}: carbon content of living phytomass
C_s: carbon content of soil
τ_s: soil turnover time
T_s: surface temperature

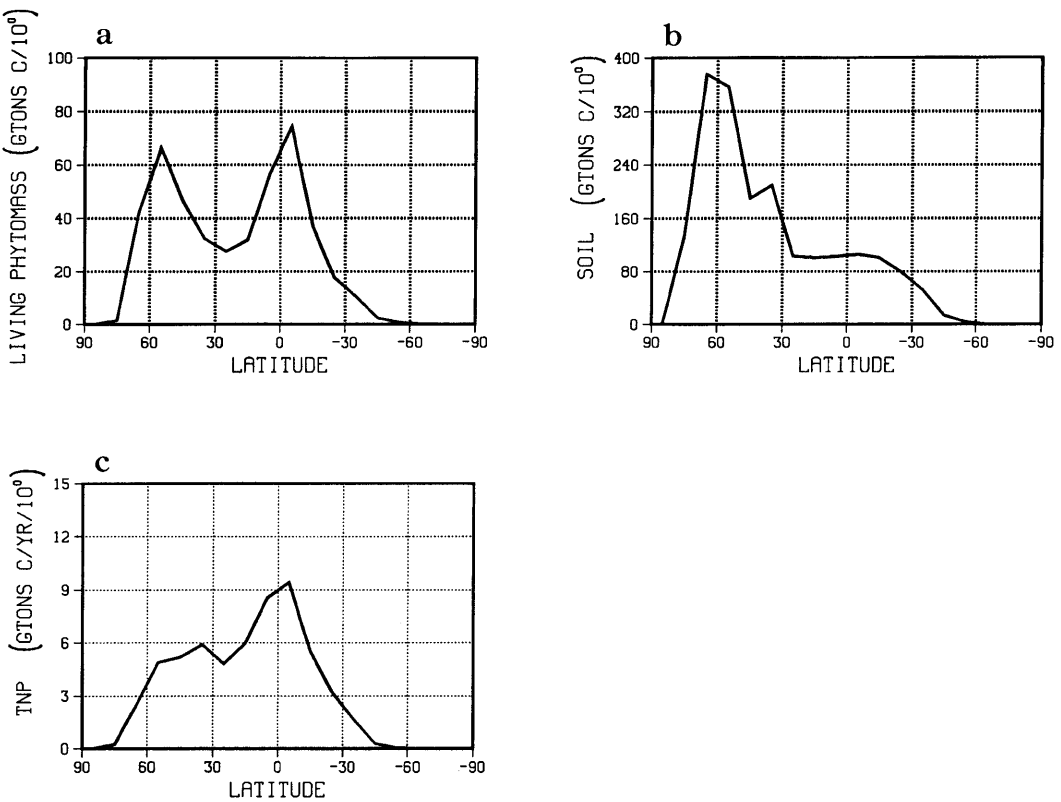

Fig. 4. Latitudinal distribution of the annually averaged (a) living phytomass carbon content, (b) soil carbon content, and (c) TNP under steady state condition with $\beta=0$. Units are in Gtons C per 10° latitude zone for (a) and (b), while Gtons C yr^{-1} per 10° latitude zone for (c).

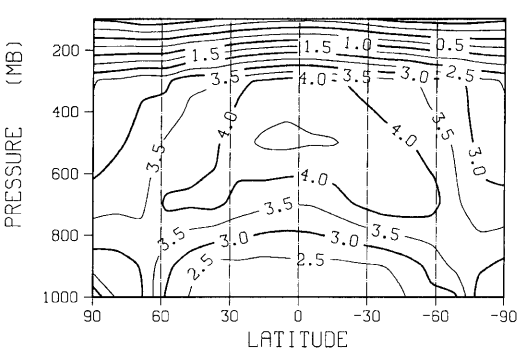

Fig. 5. Latitude-height distribution of the atmospheric annual temperature increase (°C) after 150 years of perturbed simulation (with $\beta=0$) from its initial steady state distribution.

radiative cooling by the increased CO_2 concentration there. The tropical warming in the midtroposphere is mainly due to the enhanced water vapour feedback. The overall tropospheric warming is about 2.8°C, while the corresponding value for the surface is 2.5°C.

Distribution of the annually averaged CO_2 increase in the atmosphere at the end of the perturbation (not shown) shows an interhemispheric gradient of about 18 ppm at the surface. Globally averaged atmospheric concentration has increased from its initial 334 ppm to 864 ppm, an increase of 530 ppm (1127 Gtons C). Compared to the 470 ppm increase had all the 1000 Gtons of carbon emitted over the 150 year period stayed in the atmosphere, the increase constitutes about 13% enhancement of the atmospheric CO_2 increase.

Temporal evolution of the globally averaged ΔTNP, ΔF_{sr}, and ΔNEP for $\beta = 0.0$ are shown in Fig. 6. There is an initial exponential growth in TNP and F_{sr}, becoming linear in the last 50 years or so. For the entire 150-year period, $\Delta F_{sr} > \Delta$TNP, producing negative ΔNEP.

Latitudinal changes in TNP and F_{sr} after 150 years are shown in Fig. 7. The increase in TNP is distributed across the latitude zones at about 0.2 Gtons C yr^{-1} per 10° latitude zone in the northern hemisphere as well as in the tropics. Total global increase in TNP is about 2.3 Gtons C yr^{-1}. This result is consistent with that obtained by Melillo et al. (1993) and Rotmans and Den Elzen (1993) who found that the effect of climate change on global estimate of NPP is negligible. In comparison, average increase in the soil carbon release is

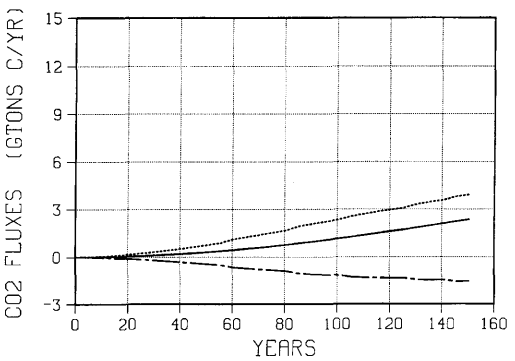

Fig. 6. Temporal evolution of the globally averaged TNP (solid), F_{sr} (dash) and NEP (dot-dash) for $\beta = 0.0$. Units are in Gtons C yr^{-1}.

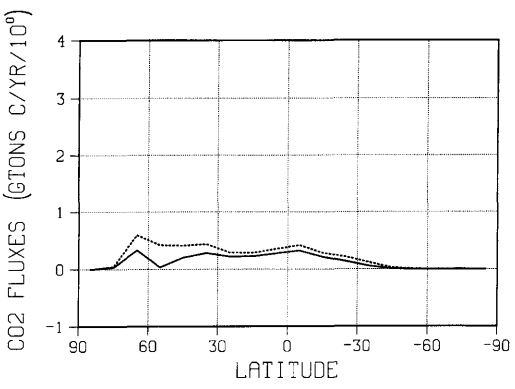

Fig. 7. Latitudinal changes in TNP (solid) and F_{sr} (dash) at the end of the perturbation for $\beta = 0$. Units are in Gtons C yr^{-1} per 10° latitude zone.

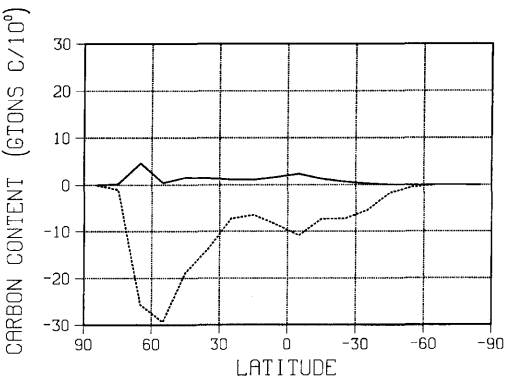

Fig. 8. Latitudinal changes in the carbon contents of the living phytomass (solid) and the soil (dash) at the end of the perturbation for $\beta = 0$. Units are in Gtons C per 10° latitude zone.

about 0.5 Gtons C yr^{-1} per 10° latitude zone in the northern hemisphere, with a slight enhancement in the high latitudes. Soil respiration has changed from a global release of 58 Gtons C yr^{-1} to almost 62 Gtons C yr^{-1}, an increase of 4 Gtons C yr^{-1} due to climatic change response only.

Latitudinal changes in the carbon contents of the living phytomass and the soil are displayed in Fig. 8. Over the 150 years of model integration, the total carbon content of the living phytomass has increased by about 17 Gtons C to 466 Gtons C, while the carbon content of the soil has decreased by about 144 Gtons C to 1790 Gtons C. Much of the soil carbon loss appears to take place around 60°N. The global soil carbon loss is about 14% of the total anthropogenic CO_2 emitted into the atmosphere. This is interestingly close to a value of 19% obtained by Jenkinson et al. (1991) who used a more "realistic" fossil fuel CO_2 release over a 60-year period. (The degree of closeness of the two results warrants a further detail study of these two different approaches.) A significant amount of the soil carbon loss occurs in the northern hemisphere high latitudes. The net loss is 144–17 = 127 Gtons of carbon from the land biosphere to the atmosphere.

If there is no fertilization effect, and the land biosphere is allowed to respond only to changes in climate parameters (Rn in equation (7), and T in eq. (11)), then the land biosphere, through enhanced release of carbon from the soil, would act as a net source of CO_2 into the atmosphere, consistent with the findings of Jenkinson et al.

(1991). On a global basis, this source amounts to about 1.6 Gtons C yr^{-1} on the 150th model year, amounting to about 12% of the anthropogenic emission rate.

3.2. *Experiment II: fertilization factor* $\beta = 0.3$

In this experiment, we set the fertilization factor $\beta = 0.3$, allowing NPP to respond to the increasing CO_2 content in the atmosphere. Assuming other major nutrients such as phosphorus and nitrogen to be nonlimiting, increasing ambient CO_2 concentration would result in a logarithmic increase in NPP (Keeling, 1973). The initial steady state of the model for Experiment II is similar to the one obtained for Experiment I, with the average atmospheric CO_2 concentration of about 334 ppm.

Annual temperature increase in the atmosphere after 150 years of perturbation is displayed in Fig. 9. Distribution of the warming in the atmosphere is qualitatively similar to the one in Experiment I; however, the increase is less, primarily due to the lesser amount of CO_2 retained by the atmosphere. The globally averaged tropospheric warming is about 2.2°C, with the corresponding surface warming of 1.9°C.

Distribution of the CO_2 increase in the atmosphere shows an interhemispheric gradient at the surface of about 10 to 12 ppm. Globally averaged atmospheric concentration has changed to 700 ppm, an increase of about 366 ppm from its initial steady state concentration of 334 ppm. Thus, in contrast to the results of Experiment I, about 210 of the 1000 Gtons C emitted into the atmosphere have been transferred to the land biosphere, making it a significant sink for excess

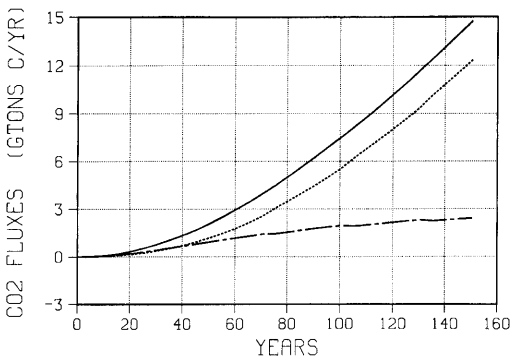

Fig. 10. Same as Fig. 6, except for $\beta = 0.3$.

atmospheric CO_2 when it is allowed to respond directly to the increasing atmospheric CO_2 through the fertilization effect.

Fig. 10 shows a very impressive response of the land carbon cycle to changes in the atmospheric CO_2 concentration in Experiment II. In contrast to Experiment I, globally averaged $\Delta TNP > \Delta F_{sr}$ throughout the 150-year period, the difference becoming time invariant in the latter stages of the integration. This is reflected in the ΔNEP curve.

Latitudinal changes in TNP and F_{sr} after 150 years for Experiment II are shown in Fig. 11. Dramatic impact of the CO_2 fertilization effect on the land biosphere carbon fluxes are clearly seen in the figure, in contrast to the relatively small impact due to climatic changes alone (Fig. 7). The increase in TNP is quite significant throughout the northern hemisphere, with a maximum in the tropics. The total global increase in TNP is about 15.5 Gtons C yr^{-1}, compared to 2.3 Gtons C yr^{-1}

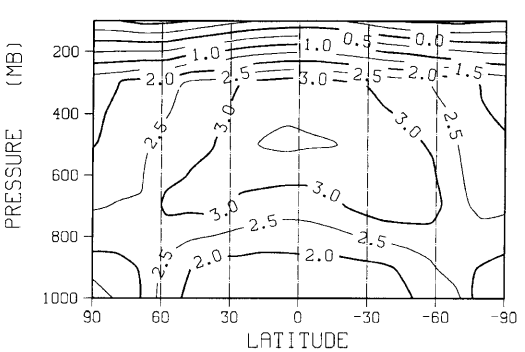

Fig. 9. Same as Fig. 5, except for $\beta = 0.3$.

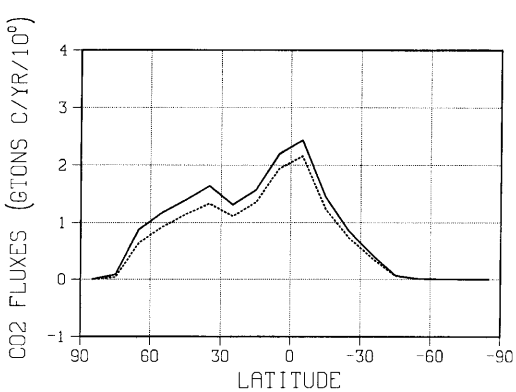

Fig. 11. Same as Fig. 7, except for $\beta = 0.3$.

in Experiment I. This increase of about 27% in TNP from its steady state value is comparable to the 20–25% increase in NPP obtained by Melillo et al. (1993). A corresponding value for the soil respiration increase is around 13 Gtons C yr^{-1}, distributed latitudinally in a same functional form as TNP, since the magnitude of soil release is now dominated by the size of the soil carbon content (eq. (7)). The soil carbon content in turn is determined by the difference between F_{sr} and the litterfall rate, the latter being a function of NPP. With the CO_2 fertilization in effect, the land biosphere becomes a net sink of about 2.5 Gtons C yr^{-1}.

In 150 years, the total carbon content of the living phytomass has increased by about 109 Gtons C to 559 Gtons C, while the carbon content of the soil has also increased by over 100 Gtons C to 2093 Gtons C. Latitudinal distribution of this gain is shown in Fig. 12 for the living phytomass and the soil. Much of the increase in the living phytomass occurs in the northern hemisphere high latitude region and in the tropics. The increase in the soil carbon content occurs predominantly in the mid to low latitude northern hemisphere region; compare this to the high latitude soil carbon loss in Experiment I.

In Fig. 13 we show the impact of the fertilization effect on limiting the increase in the globally averaged atmospheric CO_2 concentration. In the case of no fertilization ($\beta=0$), the atmospheric CO_2 concentration rises exponentially by about 530 ppm after 150 years of model integration, during which time a total of 1000 Gtons C were linearly added to the atmosphere. With $\beta=0.3$, the increase is limited to about 360 ppm. Thus, the fertilization effect, as modelled in this study, reduces the atmospheric CO_2 increase by 32% after 150 years.

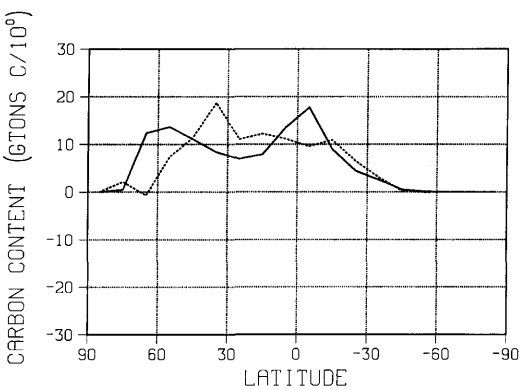

Fig. 12. Same as Fig. 8, except for $\beta=0.3$.

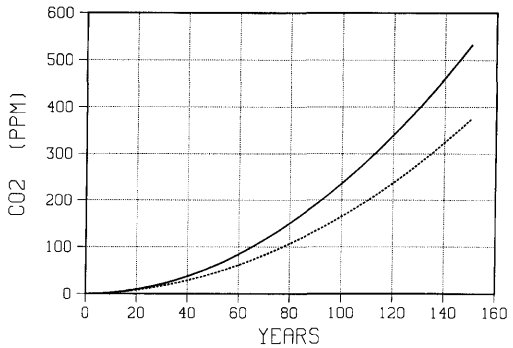

Fig. 13. Globally averaged rise in the atmospheric CO_2 concentration during the 150-year model integration for $\beta=0$ (solid) and $\beta=0.3$ (dash).

4. Conclusions

We have presented the results of 2 numerical experiments to determine the response of a land biosphere to a linearly increasing input of carbon totalling 1000 Gtons C into the atmosphere over a 150 year period. In one experiment, the fertilization factor in NPP is specified to be zero, forcing the land biosphere to respond to physical climatic changes only. At the end of 150 years, globally averaged TNP has increased by about 2.3 Gtons C yr^{-1}. Soil respiration, on the other hand, has increased by 4 Gtons C yr^{-1} responding mainly to an increase in the surface temperature caused by the CO_2 greenhouse effect. Responding only to changes in the physical climate parameters therefore causes the land biosphere to become a weak source of CO_2 for the atmosphere, amounting to about 12% of the anthropogenic emission after 150 years. Global carbon content of the living phytomass increases by 17 Gtons C, while that of the soil decreases by 144 Gtons C. Much of the soil carbon loss takes place in the high northern hemisphere latitudes.

With the fertilization factor $\beta=0.3$ in the second experiment, globally averaged TNP increases by 15.5 Gtons C yr^{-1}, while the soil release increases by around 13 Gtons C yr^{-1}, making the land

biosphere a net sink after 150 years of model integration. A net global uptake of 3 Gtons C yr^{-1} by the land biosphere after 150 years constitutes an absorption of CO_2 equal to about 22% of the anthropogenic emission. Global carbon contents of the living phytomass and the soil increase by 109 Gtons C and 103 Gtons C, respectively. Much of the increase in the living phytomass occurs in the northern hemisphere high latitude region and in the tropics. The increase in the soil carbon content occurs mainly in the mid- to low-latitude regions in the northern hemisphere. Therefore, the latitudinal distribution of the land carbon cycle response for $\beta = 0.3$ is quite different from its response for $\beta = 0$.

We have thus found that the biogeochemical response of the carbon content of the land biosphere is more sensitive to changes in the atmospheric carbon content itself than to changes in the physical climate parameters, in agreement with Rotmans and Den Elzen (1993). A relatively small net movement of carbon from the land biosphere to the atmosphere takes place when responding only to climatic changes. A significant reverse shift in the carbon transfer takes place when the carbon fertilization feedback is included, making the land biosphere a major net sink for the excess atmospheric CO_2. The qualitative aspect of these results appears to be rather robust and model independent. Thus, assuming other major nutrients to be globally nonlimiting, the degree of responsiveness of the land biosphere to the increasing atmospheric CO_2 concentration warrants a much more concerted effort in trying to increase our understanding of the carbon cycling on land, and of the very real potential role of the land biosphere as a significant "missing" sink.

5. Acknowledgements

The work was made possible by financial support from the Panel of Energy Research and Development (PERD) Programs administered by the Department of Energy, Mines and Resources, Canada. The authors are also grateful to Dr. H. Seino of the National Institute of Agro-Environment Sciences, Tsukuba, Japan for encouragement and very useful discussions. Also, thoughtful comments and suggestions by anonymous reviewers certainly helped to improve the paper.

6. Appendix A

Seasonal functions of litterfall

The variables of the 11 equations are:
SSONi = daily litterfall as percent of annual litterfall, and T = day of year.

1. No strong seasonality:-
   $SSON1 = 100/365$,
2. Conifers north:-
   $SSON2N = 0.1655$, $T < 210$;
   $SSON2N = 1.2/(((T-250)/16.0)^2+1)$,
   $210 \leqslant T \leqslant 275$;
   $SSON2N = 0.9084 - 2.0353 \times 10^{-3}\ T$, $T > 275$.
3. Conifers south:-
   $SSON2S = 0.4402 - 3.8241 \times 10^{-4}\ T$, $T < 30$;
   $SSON2S = 0.7/(((T-100)/36.49)^2+1)$,
   $30 \leqslant T \leqslant 150$;
   $SSON2S = 0.3006 - 3.8241 \times 10^{-4}\ T$, $T > 150$.
4. Temperate forests north:-
   $SSON3N = 0.0918 + 7.1019 \times 10^{-4}\ T$,
   $T < 260$;
   $SSON3N = 1.4/(((T-290)/14.88)^2+1)$,
   $260 \leqslant T \leqslant 350$;
   $SSON3N = -0.1674 + 7.1019 \times 10^{-4}\ T$,
   $T > 350$.
5. Temperate forests south:-
   $SSON3S = 0.2238 - 2.0392 \times 10^{-4}\ T$, $T < 240$;
   $SSON3S = 0.7/(((T-300)/34.62)^2+1)$,
   $240 \leqslant T \leqslant 350$;
   $SSON3S = 0.2982 + 2.0392 \times 10^{-4}\ T$,
   $T > 350$.
6. Subtropical forests north:-
   $SSON4N = 0.5/(((T+45)/83.84)^2+1)$, $T \leqslant 85$;
   $SSON4N = 0.1342 + 1.49 \times 10^{-4}\ T$,
   $85 < T < 200$.
   $SSON4N = 0.5/(((T-320)/83.84)^2+1)$,
   $T \leqslant 200$;
7. Subtropical forests south:-
   $SSON4S = 0.5/(((T-120)/83.84)^2+1)$,
   $T \leqslant 250$;
   $SSON4S = 0.1096 + 1.49 \times 10^{-4}\ T$, $T > 250$.

8. Tropical forests north:-
   $SSON5N = 0.2184 + 2.691 \times 10^{-4}\ T,\ T < 10.$
   $SSON5N = 0.45/(((T-100)/88.46)^2+1),$
   $10 \leqslant T \leqslant 210;$
   $SSON5N = 0.1202 + 2.691 \times 10^{-4}\ T,\ T > 210.$
9. Tropical forests south:-
   $SSON5S = 0.45/(((T+75)/88.46)^2+1),$
   $T < 35;$
   $SSON5S = 0.1673 + 2.6903 \times 10^{-4}\ T,$
   $35 \leqslant T \leqslant 200.$
   $SSON5S = 0.45/(((T-290)/88.46)^2+1),$
   $T > 200;$
10. Mediterranean north:-
    $SSON6N = 0.1144 + 1.2721 \times 10^{-4}\ T,\ T < 65;$
    $SSON6N = 1.5/(((T-130)/19.4)^2+1),$
    $65 \leqslant T \leqslant 205;$
    $SSON6N = 0.0680 + 1.2721 \times 10^{-4}\ T,$
    $T > 205.$
11. Mediterranean south:-
    $SSON6S = 1.0/(((T+30)/33.4)^2+1),\ T < 75;$
    $SSON6S = 0.0836 + 1.0983 \times 10^{-4}\ T,$
    $75 \leqslant T \leqslant 240.$
    $SSON6S = 1.0/(((T-335)/33.4)^2+1),$
    $T > 240;$

7. Appendix B

Coefficients of functions relating rate of soil respiration to ground level temperature

The general form of the function is given in eq. (11). For tropical and subtropical seasonal forests, savanna and woodlands, the dry-season equation is used when precipitation is below 1/86400 kg m^{-2} s^{-1} and ground-level temperature is higher than 303K.

Ecosystems	a	b	Ecosystem complex*	Data sources
Taiga	5.2369	−3948.909	1, 2, 14	Gordon et al. (1987); Schlentner and Van Cleve (1985)
Conifer	14.3134	−6516.663	3	Nakane et al. (1983; 1984; 1986); Vogt et al. (1980); Steubing (1977)
Temperate mixed	15.817	−7001.303	4	Nakane (1980); Witkamp (1966)
Temperate broad-leaved	21.1831	−8578.366	5	Edwards (1975); Edwards et al. (1973); Ellis (1969); Froment (1972); Nakane (1980); Stuebing (1977)
Tropical evergreen	19.9569	−8208.832	6	Maggs and Hewett (1990); Medina and Zelwer (1972); Nakane (1980); Ogawa (1978)
Tropical seasonal (wet)	17.2967	−7668.538	7, 8, 13	Yoda and Nishioka (1982); Rajvanshi and Gupta (1986)
Tropical seasonal (dry)	−17.2795	2605.762	7, 8	Yoda and Nishioka (1982); Rajvanshi and Gupta (1986)
Tropical montane	10.0297	−5728.279	9, 31	De Santo et al. (1976)
Mediterranean	17.2476	−7471.101	10, 11	Lossaint (1973); O'Connell (1987)
Temperate woodland	24.8695	−9604.524	15, 16, 31	Ellis (1974); Anderson (1973)
Cool cropland	10.2533	−5466.049	18, 19	Buyanovsky et al. (1986; 1987); Ellis (1974)
Warm cropland	1.4261	−3132.639	17, 20, 29	Singh and Shekhar (1986)

Cool grassland	17.1889	−7672.136	12, 21, 23, 24, 27	Coleman (1973); de Jong et al. (1979); Hunt (1977); Kucera and Kirkham (1971)
Warm grassland	13.1588	−6502.693	22, 28	Gupta and Singh (1981)
Wooded tundra	11.0406	−5880.771	25	Svensson et al. (1975)
Tundra	19.4423	−8214.637	26, 33	Peterson and Billings (1975); Billings et al. (1978)
Cool wetlands	13.6428	−7062.36	30	Reiners (1968), Lieth and Ouellette (1962)

* See Table 1 for type of ecosystem complex.

REFERENCES

Ajtay, G. L., Ketner, P. and Duvigneaud, P. 1979. Terrestrial primary production and phytomass. In: *The global carbon cycle* (B. Bolin, E. T. Degens, S. Kempe, and P. Ketner, eds.). John Wiley & Sons, Chichester, U.K., 129–181.

Anderson, J. M. 1973. Carbon dioxide evolution from two temperate deciduous woodland soils. *J. Appl. Ecol.* **10**, 361–378.

Billings, W. D., Peterson, K. M. and Shaver, G. R. 1978. Growth, turnover, and respiration rates of roots and tillers in tundra graminoids. In: *Vegetation and production ecology of an Alaskan Arctic tundra* (I. L. Tieszen, ed.). Springer-Verlag, New York, 415–434.

Bray, J. R. and Gorham, E. 1964. Litter production in forests of the world. *Adv. Ecol. Res.* **2**, 101–157.

Broecker, W. S., Takahashi, T., Simpson, H. J. and Peng, T.-H. 1979. Fate of fossil fuel carbon dioxdie and the global carbon budget. *Science* **206**, 409–418.

Broecker, W. S., Peng, T.-H. and Engh, R. 1980. Modelling the carbon system. In: Carbon dioxide effects research and assessment program. *Proceedings of the Carbon dioxide and climate research program Conference* (L. E. Schmitt, ed.). Dept. of Energy, Washington, D.C., 43–99.

Budyko, M. I. 1974. *Climate and life.* Academic Press, London. 508 p.

Buyanovsky, G. A., Kucera, C. L. and Wagner, G. H. 1987. Comparative analysis of carbon dynamics in native and cultivated ecosystems. *Ecology* **68**, 2023–2031.

Buyanovsky, G. A., Wagner, G. H. and Gantzer, C. J. 1986. Soil respiration in a winter wheat ecosystem. *Soil Sci. Soc. Amer. J.* **50**, 338–343.

Chan, D., Higuchi, K. and Lin, C. A. 1995. The sensitivity of the simulated normal and enhanced CO_2 climates to different heat transport parameterizations in a 2-dimensional multilevel energy balance model. *J. Climate* **8**, 844–852.

Coleman, D. C. 1973. Soil carbon balance in a successional grassland. *Oikos* **24**, 195–199.

De Jong, E., Redmann, R.E. and Ripley, E.A. 1979. A comparison of methods to measure soil respiration. *Soil Sci.* **127**, 300–306.

De Santo, V. A., Alfani, A. and Sapio, S. 1976. Soil metabolism in beech forests of Monte Taburno (Campania Apennines). *Oikos* **27**, 144–152.

Edwards, N. T. 1975. Effects of temperature and moisture on carbon dioxide evolution in a mixed deciduous forest floor. *Soil Sci. Amer. Proc.* **39**, 361–365.

Edwards, N. T. and Sollins, P. 1973. Continuous measurements of carbon dioxide evolution from partitioned forest floor components. *Ecology* **54**, 406–412.

Efimova, N. A. 1976. Maps of natural vegetation cover productivity on the continents. *Bot. J.* **61**, 1641–1657. (in Russian).

Emanuel, W. R., Shugart, H. H. and Stevenson, M. P. 1985. Climatic change and the broad-scale distribution of terrestrial ecosystem complexes. *Climate Change* **7**, 29–43.

Ellis, R. C. 1969. The respiration of the soil beneath some Eucalyptus forest stands as related to the productivity fo the stands. *Aust. J. Soil Res.* **69**, 349–357.

Ellis, R. C. 1974. The seasonal pattern of nitrogen and carbon mineralization in forest and pasture soils in southern Ontario. *Can. J. Soil Sci.* **54**, 15–28.

Froment, A. 1972. Soil respiration in a mixed oak forest. *Oikos* **23**, 273–277.

Gillette, D. and Box, E. O. 1986. Modeling seasonal changes of atmospheric carbon dioxide and carbon 13. *J. Geophys. Res.* **91**, 5287–5304.

Gordon, A. M., Schlentner, R. E. and Van Cleve, K. 1987. Seasonal patterns of soil respiration and CO_2 evolution following harvesting in the white spruce forests of interior Alaska. *Can. J. For. Res.* **17**, 304–310.

Gupta, S. R. and Singh, J. S. 1981. Soil respiration in a tropical grassland. *Soil Biol. Biochem.* **13**, 261–268.

Harrison, K., Broecker, W. and Bonani, G. 1993. A strategy for estimating the impact of CO_2 fertilization on soil carbon storage. *Global Biogeochem. Cycles* **7**, 69–80.

Harvey, L.D.D. 1989. Effect of model structure on the response of terrestrial biosphere models to CO_2 and temperature increases. *Global Biogeoche. Cycles* **3**, 137–153.

Hunter, H. W. 1977. A simuation model for decomposition in grassland. *Ecology* **58**, 469–484

IPCC Report. 1990. *Climate change. The IPCC Scientific Assessment.* (J.T. Houghton, B. A. Callander, and S. K. Varney, eds.). Cambridge University Press, Cambridge, U.K., 365 p.

Jenkinson, D. S., Adams, D. E. and Wild, A. 1991. Model estimates of CO_2 emissions from soil in response to global warming. *Nature* **351**, 304–306.

Keeling, C. D. 1973. The carbon dioxide cycle: reservoir models to depict the exchange of atmospheric carbon dioxide with the oceans and land plants. In: *Chemistry of the lower atmosphere* (S.I. Rasool, ed.). Plenum Press, New York, 251–329.

Kempe, S. 1979. Carbon in the freshwater cycle. In: *The global carbon cycle* (B. Bolin, E. T. Degens, S. Kempe, and P. Ketner, eds.). John Wiley & Sons, Chichester, U.K., 317–342.

Kohlmaier, G. H., Bröhl, H., Siré, E. O., Plöchl, M. and Revelle, R. 1987. Modelling stimulation of plants and ecosystem response to present levels of excess atmospheric CO_2. *Tellus* **39B**, 155–170.

Kucera, C. L. and Kirkham, D.R. 1971. Soil respiration studies in tallgrass Prairie in Missouri. *Ecology* **52**, 912–915.

Lieth, H. 1975. Modeling the primary productivity of the world. In *Primary productivity of the biosphere* (H. Lieth and R.H. Whittaker, eds.). Springer-Verlag, New York, 237–263.

Lieth, H. and Ouellette, R. 1962. Studies on the vegetaion of the Gaspe Peninsula. II: The soil respiration of some plant communities. *Can. J. Bot.* **40**, 127–140.

Lloyd, J., and Taylor, J.A. 1994. On the temperature dependence of soil respiration. *Functional Ecology* **8**, 315–232.

Lossaint, P. 1973. Soil-vegetation relationships in Mediterranean ecosystems of southern France. In: *Mediterranean type ecosystmes: origin and structure* (F. Costri and H.A. Mooney, eds.). Springer-Verlag, New York, 199–230.

Maggs, J. and Hewett, B. 1990. Soil and litter respiration in rainforests of contrasting nutrient status and physiognomic structure near Lake Eacham, northeast Queensland. *Aust. J. Ecol.* **15**, 329–336.

Matthews, E. 1983. Global vegetation and land use: new high-resolution data bases for climate studies. *J. Clim. Appl. Meteor.* **22**, 474–488.

Matthews, E. 1984. *Vegetation, land-use and seasonal albedo data sets: documentation of archived data tape.* NASA Technical Memorandum 86107. Goddard Space Flight Center, Institute for Space Studies, New York, 12 p.

Medina, E. and Zelwer, M. 1972. Soil respiration in tropical plant communities. In: *Tropical ecology, with emphasis on organic matter production* (P. Golley and F.B. Golley, eds.). University of Georgia Press, Athens, Georgia, USA, 245–269.

Melillo, J. M., McGuire, A. D., Kicklighter, D. W., Moore III, B., Vorosmarty, C. J. and Schloss, A. L. 1993. Global climate change and terrestrial net primary production. *Nature* **363**, 234–240.

Nakane, K. 1980. Comparative studies of cycling of soil organic carbon in three primeval moist forests. *Jap. J. Ecol.* **30**, 155–172.

Nakane, K., Tsubota, H. and Yamamoto, M. 1984. Cycling of soil carbon in a Japanese red pine forest. I. Before a clear-felling. *Bot. Mag.* (Tokyo) **97**, 39–60.

Nakane, K., Tsubota, H. and Yamamoto, M. 1986. Cycling of soil carbon in a Japanese red pine forest. II. Changes occurring in the first year after a clear-felling. *Ecol. Res.* **1**, 47–58.

Nakane, K., Yamamoto, M. and Tsubota, H. 1983. Estimation of root respiration rate in a mature forest ecosystem. *Jap. J. Ecol.* **33**, 397–408.

Newton, C. W. 1972. Southern hemisphere general circulation in relation to global energy and momentum balance requirements. In *Meteorology of the Southern Hemisphere. Meteorol. Monogr.* **13**, 215–240. American Meteorological Society, Boston.

O'Connell, A.M. 1987. Litter decomposition, soil respiration and soil chemical and biochemical properties at three constrasting sites in karri (*Eucalyptus diversicolor F. Muell.*) forests of south-western Australia. *Aust. J. Ecol.* **12**, 31–40.

Ogawa, H. 1978. Litter production and carbon cycling in Pasoh forest. *Malay. Nat. J.* **30**, 367–373.

Olson, J. S., Pfuderer, H. A. and Chan, Y.-H. 1978. *Changes in the global carbon cycle and the biosphere.* ORNL/EIS-109. Oak Ridge National Laboratory, Oak Ridge, Tennessee.

Olson, J. S., Watts, J. A. and Allison, L. J. 1983. *Carbon in live vegetation of major world ecosystems.* ORNL-5862. Oak Ridge National Laboratory, Oak Ridge, Tennessee, 164 p.

Olson, J. S., Watt, J. A. and Allison, L. J. 1985. *Major World Ecosystem Complexes Ranked by Carbon in Live Vegetation: A Database.* NDP-017. Oak Ridge National Laboratory, Oak Ridge, Tennessee.

Peng. L., Chou, M.-D. and Arking, A. 1987. Climate warming due to increasing atmospheric CO_2: simulations with a multilayer coupled atmosphere-ocean seasonal energy balance model. *J. Geophys. Res.* **92**, 5505–5521.

Peterson, K. M. and Billings, W. D. 1975. Carbon dioxide flux from tundra soils and vegetation as related to temperature at Barrow, Alaska. *Amer. Midl. Natur.* **94**, 88–98.

Potter, C. S., Randerson, J. T., Field, C. B. Matson, P. A., Vitousek, P. M., Mooney, H. A. and Klooster, S. A. 1993. Terrestrial ecosystem production. A process model based on global satellite and surface data. *Global Biogoechem. Cycles* **7**, 811–841.

Raich, J. W. and Schlesinger, W. H. 1992. The global carbon dioxide flux in soil respiration and its relationship to vegetation and climate. *Tellus* **44B**, 81–99.

Rajvanshi, R. and Gupta, S. R. 1986. Soil respiration and carbon balance in a tropical *Dalbergia sissoo* forest ecosystem. *Flora* **178**, 251–260.

Reiners, W. A. 1968. Carbon dioxide evolution from the floor of three Minnesota forests. *Ecology* **49**, 479–483.

Rotmans, J. and Den Elzen, M. G. J. 1993. Modelling feedback mechanisms in the carbon cycle: balancing the carbon budget. *Tellus* **45B**, 301–320.

Schlentner, R. E. and Van Cleve, K. 1985. Relationships between CO_2 evolution from soil, substrate temperature, and substrate moisture in four mature forest types in interior Alaska. *Can. J. For. Res.* **15**, 97–106.

Schlesinger, W. H. 1977. Carbon balance in terrestrial detritus. *Ann. Rev. Ecol. Syst.* **8**, 51–81.

Schlesinger, W. H. 1984. Soil organic matter: a source of atmosphere CO_2. In: *The role of terrestrial vegetation in the global carbon cycle: measurement by remote sensing* (G. M. Woodwell, ed.). John Wiley & Sons, Chichester, U.K., 111–130.

Schutz, C. and Gates, W. L. 1974. *Global climate data for surface, 800 mb, and 400 mb.* Rep. R-1425-ARPA, Rand Corp., Santa Monica, Calif.

SCOPE 16, 1981. *Carbon cycle modelling.* (B. Bolin, ed.). John Wiley & Sons, Chichester, U.K., 390 p.

Seino, H. and Uchijima, Z. 1985. Agroclimatic evaluation of net primary productivity of natural vegetation. (2) Assessment of total net primary production in Japan. *J. Agr. Meteoro.* **41**, 139–144.

Seino, H. and Uchijima, Z. 1988. *Mesh maps of net primary productivity of natural vegetation of Japan.* Nat. Inst. Agro-Environ. Sc., 131 p.

Seino, H. and Uchijima, Z. 1992. Global distribution of net primary productivity of terrestrial vegetation. *J. Agr. Meteoro.* **48**, 39–48.

Singh, J. S. and Gupta, S. R. 1977. Plant decomposition and soil respiration in terrestrial ecosystems. *Bot. Rev.* **43**, 449–528.

Singh, K. P. and Shekhar, C. 1986. Seasonal pattern of total soil respiration, its fractionation and soil carbon balance in a wheat-maize rotation cropland at Varanasi. *Pedobiologia* **29**, 305–318.

Steubing, L. 1977. Soil microbial activity under beech and spruce stances. *Nat. Can. (Que.)* **104**, 143–150.

Stone, P. H. 1974. The meridional variation of the eddy heat fluxes by baroclinic waves and their parameterization. *J. Atmos. Sci.* **31**, 444–456.

Svensson, B. H., Veum, A. K. and Kjelvik, S. 1975. Carbon losses from tundra soils. In: *Fennoscandian tundra ecosystems. Part I. Plants and micro-oraganisms* (F.E. Wielgolaski, ed.). Springer-Verlag, New York, 279–285.

Tans, P., Fung, I. and Takahashi, T. 1990. Observational constraints on the global atmospheric CO_2 budget. *Science* **247**, 1431–1438.

Uchijima, Z. and Seino, H. 1985. Agroclimatic evaluation of net primary productivity of natural vegetations (1). Chikugo model for evaluating net primary productivity. *J. Agr. Meteoro.* **40**, 343–352.

Uchijima, Z. and Seino, H. 1987. *Maps of net primary productivity of natural vegetation on continents.* Special Report of National Institute of Agro-Environment Sciences and Kyushu National Agriculture Experimental Station 102.

Uchijima, Z. and Seino, H. 1988a. An agroclimatic method of estimating net primary productivity of natural vegetation. *J. Agr. Res. Quat.* **21**, 244–250.

Uchijima, Z. and Seino, H. 1988b. Probable effects of CO_2-induced climate change on agroclimatic resource and net primary productivity in Japan. *Bull. Natl. Instl. Agro-Eniron. Sci.* **4**, 67–88.

Vogt, K. A., Edmonds, R. L., Antos, G. C. and Vogt, D. J. 1980. Relationships between CO_2 evolution, ATP concentrations and decomposition in four forest ecosystems in western Washington. *Oikos* **35**, 72–79.

Vogt, K. A., Grier, C. C. and Vogt, D. J. 1986. Production, turnover, and nutrient dynamics of above- and below ground detritus of world forests. *Adv. Ecol. Res.* **15**, 303–377.

Whittaker, R. H. and Marks, P.L. 1975. Methods of assessing terrestrial productivity. In: *Primary productivity of the biosphere* (H. Lieth and R. H. Whittaker, eds.). Springer-Verlag, New York, 55–118.

Witkamp, M. 1966. Rates of carbon dioxide evolution from the forest floor. *Ecology* **47**, 492–494.

Yoda, K. and Nishioka, M. 1982. Soil respiration in dry and wet seasons in a tropical dry-evergreen forest in Sakaerat, NE Thailand. *Jap. J. Ecol.* **32**, 539–541.

Zinke, P. J., Stangenberger, A. G., Post, W. M., Emanuel, W. R. and Olson, J. S. 1984. *Worldwide organic soil carbon and nitrogen data.* ORNL/TM-8857. Oak Ridge National Laboratory, Oak Ridge, Tennessee, 141 p.